THE SYRINX: NATURE'S HYBRID WIND INSTRUMENT

Tamara Smyth, Julius O. Smith

Center for Computer Research in Music and Acoustics
Department of Music, Stanford University
Stanford, California 94305-8180 USA
tamara@ccrma.stanford.edu, jos@ccrma.stanford.edu

Abstract

This research presents a model of the avian vocal tract, implemented using waveguide synthesis and numerical methods. The vocal organ of the songbird, the syrinx, has a unique topography of acoustic tubes (a trachea with a bifurcation at its base) making it a novel subject for waveguide synthesis. In the upper region of the two bifid bronchi lies a nonlinear vibrating membrane—the primary resonator in sound production. The model of the membrane displacement, and the resulting pressure through the constriction created by the membrane motion, is derived based on the Bernoulli equation for the air flow and the mechanical properties of the membrane and surrounding tissue.

1. INTRODUCTION

The pure, often high pitched, tone of the songbird is undeniably flute-like. Yet the theory that the song bird produces its sound using an aerodynamic whistle effect much like in the flute, has been widely confuted [8, 1, 2]. Rather, it has been determined that the avian vocal tract uses a nonlinear vibrating membrane as its primary excitation mechanism. The syringeal membrane, much like the vocal folds in the human vocal tract, forms a vibrating valve, the output of which is filtered by the bronchi trachea which amplify and attenuate certain harmonics of the vibrating membrane.

The modeling methods described here have been used extensively for synthesizing wind instruments. Their use in modeling the bird's vocal system provides a unique configuration of acoustic elements not found in traditional musical instruments—creating a new hybrid instrument based on a sound mechanism that has always intrigued human listeners.

2. THE AVIAN VOCAL TRACT

The syrinx is the bird's unique vocal organ. It consists of an airway—a trachea which divides into the left and right bronchus at its base (Fig. 1)—and two pressure-controlled valves made of flexible membranes, the tensions of which are altered by surrounding muscles [9]. The neural control of the muscles and the bird's respiratory mechanics both greatly contribute to how sound is modulated by the syrinx [2].

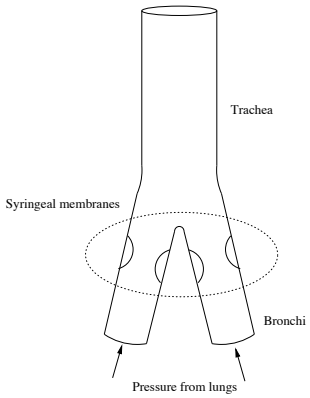

Figure 1: *The syrinx*.

Airflow in the syrinx begins from the lungs and passes through the bronchi, trachea and mouth before radiating from the beak (Fig. 4). On its way, the airflow passes through the bird's primary vocal organ, a non-linear vibrating membrane, situated just below the junction of the two bronchi with the trachea (Fig. 1).

2.1. The Syringeal Membrane

When the bird is at rest, the syringeal membrane lies flat on the wall of the bronchus. When singing begins, the membrane vibrates, with motion occurring primarily toward the opposite cartilaginous wall (Fig. 2). This creates a narrowing in the bronchus (with the possibility of closing the air passage completely), and a constriction through which the air flows.

The motion of the syringeal membrane can be described by two of the three configurations for pressure-controlled valves in acoustic tubes [4]. The three possible configurations are: 1) The reed is blown closed (as in woodwind instruments). 2) The reed is blown open (as in the human larynx). 3) The transverse model – the Bernoulli pressure causes the valve to close, perpendicular to the direction of airflow [7, 4]. Though the syrinx uses both configurations 2 and 3, as does the human voice, the third tends to be most significant and is used as the model for implementing the membrane's motion. It is interesting to note that this third configuration does not seem to be employed as significantly by traditional musical instruments [4]. A musical exploration of this model could, therefore, make new contributions to the synthesis of new sounds in computer music.

2.1.1. The Membrane Modeled as the Transverse Configuration of a Pressure Controlled Valve

In voiced song (as opposed to whistled song), the membrane is set into motion by airflow. Like any mechanical resonator, it vibrates at a frequency controlled partly by its natural frequency (determined by its mass and tension) and partly by the resonance of the air column to which which it is connected.

The model of the syringeal membrane, the nonlinearity (NL in Fig. 4), determines the pressure on the tracheal side of the constriction (p_1) based on a given input pressure (p_0) from the bronchial side.

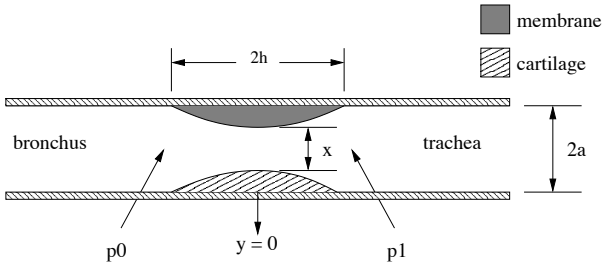

Figure 2: *The pressure-controlled valve in the syrinx.*

The nonlinear junction of the bronchi to the trachea was developed following the acoustic model by Fletcher of airflow through the syringeal constriction [3, 6]. The model has the following four key variables, all of which vary over time during sound production.

$$\begin{aligned} p_0 &\triangleq \text{pressure on the bronchial side of the constriction} \\ U &\triangleq \text{air volume flow through the syrinx} \\ x &\triangleq \text{displacement of the membrane} \\ p_1 &\triangleq \text{pressure on the tracheal side of the constriction} \end{aligned} \tag{1}$$

2.1.2. Bronchial Pressure ($\mathbf{p_0}$)

The lower bronchi are extremely short and are sufficiently modeled as having a volume (V) and an acoustic stiffness $\frac{\rho c^2}{V}$. The rate at which pressure builds up in the lower bronchus ($\frac{dp_0}{dt}$) is then proportional to the difference in volume velocity flowing *in* ($\frac{p_G - p_0}{Z_G}$) and flowing *out* (U) of the constriction.

$$\frac{dp_0}{dt} = \left(\frac{\rho c^2}{V}\right)\left(\frac{p_G - p_0}{Z_G} - U\right) \tag{2}$$

where,

$Z_G \triangleq$ impedance of the air sacs
$\rho \triangleq$ air density
$V \triangleq$ volume of the bronchus
$c \triangleq$ speed of sound (in air)

2.1.3. Volume Flow ($\mathbf{U}$*)*

Since the motion of the membrane causes varying heights in the constriction, Bernoulli's equation (3) is used to determine the pressure at a given point y:

$$p(y) = p_0 + \frac{\rho}{2}\left[v_0^2 - v(y)^2\right] \tag{3}$$

where v is the particle velocity at a given point, and is equal to the volume velocity, U, divided by the cross-section area at that point. That is,

$$v(y) = \frac{U}{2a\left[x + (a-x)(\frac{y}{h})^2\right]} \tag{4}$$

Since U likely forms a jet at $y > 0$, the pressure acting on the entire tracheal half of the membrane is equal to the pressure at the base of the upper bronchus [3]. That is, the pressure at point y = 0 is effectively p_1.

Given that the area of the constriction at point $y = 0$ is $2ax$, (3) becomes

$$p_1 = p_0 + \frac{\rho}{2}\left[\left(\frac{U}{2\pi a^2}\right)^2 - \left(\frac{U}{2ax}\right)^2\right] \tag{5}$$

which can be reduced to

$$p_1 = p_0 - \frac{\rho}{2}\left(\frac{U}{2ax}\right)^2 \tag{6}$$

when $x \ll \pi a$.

The final differential equation governing airflow is obtained by incorporating the force used to accelerate air through the syrinx [3] (this adds a pressure drop of $\frac{\rho}{2\sqrt{ax}}\frac{dU}{dt}$), and by rearranging the equation to isolate $\frac{dU}{dt}$:

$$\frac{dU}{dt} = \frac{2\sqrt{ax}}{\rho}\left(p_0 - p_1 - \frac{\rho}{8a^2x^2}U^2\right) \tag{7}$$

2.1.4. Membrane Motion ($\mathbf{x}$*)*

When x, the displacement of the membrane, is equal to zero, the membrane is touching the opposite wall, and the constriction is closed.

Fletcher writes the membrane's motion for mode n as:

$$m_n\left[\frac{d^2x_n}{dt^2} + 2\kappa\frac{dx_n}{dt} + \omega_n^2(x_n - x_0)\right] = \epsilon_n F \tag{8}$$

where

$\omega_n \triangleq$ the radian frequency of mode n
$m_n \triangleq$ the effective mass associated with mode n
$\kappa \triangleq$ the damping coefficient
$\epsilon_n \triangleq$ the coupling coefficient between F and mode n

and F is the force driving the fundamental mode of the membrane, expressed as

$$F = ah(p_0 + p_1) - \frac{2\rho U^2 h}{7(ax)^{1.5}} \quad \text{for } x > 0 \tag{9}$$

In order to account for the damping that would occur should the membrane actually touch the opposite wall, a factor E is introduced into (8). Its actual value depends on the stickiness of the contact between the membrane and the wall [3].

$$\kappa \rightarrow E\kappa \quad 10 \leq E \leq 100 \quad \text{if } x \leq 0 \tag{10}$$

When the membrane's displacement becomes very large, surrounding tissue will likely take part in the vibration [3]. To account for this, the mass m from (8) is replaced with the following term, so that the mass changes nonlinearly depending on the membrane's position (x).

$$m \rightarrow m\left(1 + \eta\left(\frac{x - x_0}{h}\right)^2\right) \tag{11}$$

The 2nd derivative of x_n is isolated by rearranging (8) and, for simplicity, the coupling coefficient (ϵ) is made equal to unity.

$$\frac{d^2 x_n}{dt^2} = \frac{\epsilon F}{m_n} - 2\kappa\frac{dx_n}{dt} - \omega^2(x_n - x_0) \tag{12}$$

2.1.5. Upper Bronchus Pressure ($\mathbf{p_1}$)

The pressure leaving the constriction (p_1) is proportional to the volume velocity (U), scaled by the characteristic impedance of the bronchus ($Z_0 = \frac{\rho c}{\pi a^2}$). In order to obtain the true pressure at the base of this section of the bronchus, the pressure due to all previous reflections must also be considered. This is taken into account with the waveguide models for the the bronchi and trachea, and the 3 port junction (see 4).

2.2. Numerical Methods

2.2.1. Backwards Difference and the Trapezoid Rule

The following so-called backward-difference equations are commonly used for numerically integrating differential equations:

$$\begin{aligned} x'[n] &= \frac{x[n] - x[n-1]}{T} \\ x''[n] &= \frac{x[n-2] - 2x[n-1] + x[n]}{T^2} \end{aligned} \tag{13}$$

where $x'[n]$ and $x''[n]$ are the first and second derivatives of $x(t)$ at $t = nT$, and T is the sampling period. Since the current model isolates the derivatives of the variables from 1 (and it is the instantaneous value of these variables that we require), these equations are more conveniently expressed as follows:

$$\begin{aligned} x[n] &= x[n-1] + x'[n]T \\ x'[n] &= x'[n-1] + x''[n]T \end{aligned} \tag{14}$$

The accuracy of the backwards-difference approximation is dependent on T (the sampling period). Specifically, it is first-order accurate in T [10]. We found via numerical simulations that this level of accuracy is not sufficient for

stability at typical audio sampling rates (e.g., $T = 1/44100$). We therefore went to a finite difference scheme which is seconod-order accurate in T.

The second-order scheme uses the trapezoid rule for numerical integration [10, 11]. It yields the following difference equations (comparable to (14)), and solves the problem of stability at audio sampling periods:

$$\begin{aligned} x[n] &= x[n-1] + (x'[n] + x'[n-1])\left(\frac{T}{2}\right) \\ x'[n] &= x'[n-1] + (x''[n] + x''[n-1])\left(\frac{T}{2}\right) \end{aligned} \tag{15}$$

2.2.2. Solving the Model Numerically

For the purpose of discussion, the model of the vibrating membrane can be reduced to the differential equations (2), (7), (12). Solving the system of equations is done as follows:

All variables and their derivatives are initialized to zero. Pressure from the the air sacs is introduced into the system by setting p_G to some value.

The derivatives of p_0, U, and x are discretized as follows:

$$\begin{aligned} p_0' &= \left(p_0' + \left(\frac{\rho c^2}{V}\right)\left(\frac{p_G - p_0}{Z_G} - U\right)\right)\frac{T}{2} \\ U' &= \left(U' + D\left(p_0 - p_1 - \frac{\rho}{8a^2x^2}U^2\right)\frac{T}{2}\right) \quad 0 < x \leq a \\ x_n'' &= \left(x_n'' + \frac{\epsilon F}{m_n} - 2\kappa\frac{dx_n}{dt} - \omega^2\left(x_n - x_0\right)\right)\frac{T}{2} \end{aligned} \tag{16}$$

In the case of membrane displacement x, the displacement is calculated for 2 modes (giving x_1 and x_2) which are added to produce the overall displacement of the membrane.

The displacement (x), and the pressure at the base of the upper bronchus (p_1), is plotted in Fig. 3 along with the audio output (taken at the top of the trachea). It is interesting to observe how the pressure (taken at both the top and bottom of the trachea) relates to the displacement of the membrane. Both pressure waves display a pulsation that clearly coincides with the frequency of the oscillating membrane. When the membrane closes the constriction completely (i.e., when $x = 0$), the amplitude of p_1 is high and its frequency is close to the resonance of a closed tube. When the membrane is open ($x > 0$), the pressure amplitude decreases and the frequency increases to the resonance of an open tube.

3. WAVEGUIDE SYNTHESIS AND THE 3-PORT PARALLEL JUNCTION

Waveguide synthesis is used to model the pressure waves in the bronchi and the trachea. Given the general solution to the 1-D wave equation:

$$p(x,t) = p^+(x - ct) + p^-(x + ct) \tag{17}$$

where the 1^{st} term is the pressure wave traveling toward the right at speed c and the 2^{nd} term is the pressure wave traveling toward the left at speed c, the 3-port junction model will receive an incoming pressure wave (P_i^+) from the two bronchi and the trachea, and will send to each an outgoing pressure wave (P_i^-).

The characteristic impedance (Z) of an acoustic tube describes the ratio of pressure (P) and volume velocity (U). It is given by:

$$\frac{P}{U} = Z = \frac{\rho c}{A} = \frac{\rho c}{\pi r^2} \tag{18}$$

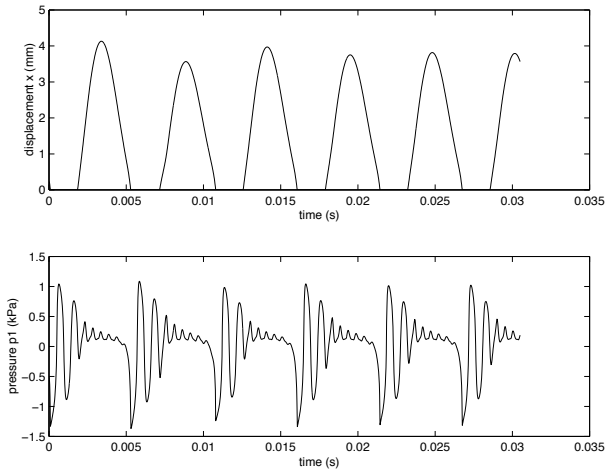

Figure 3: *Waveforms are comparable to those published by Fletcher, but use waveguides with lumped losses and a 2nd-order-error algorithm for numerical integration to achieve stable discretization at audio sampling rates.*

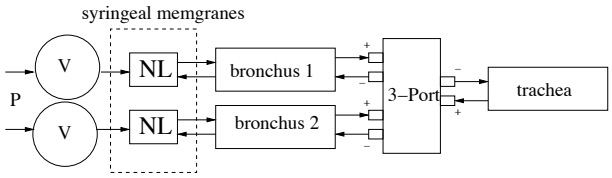

Figure 4: *Block diagram of avian vocal tract.*

where

$$\begin{aligned} \rho &\triangleq \text{air density} \\ A &\triangleq \text{cross-sectional area of the tube} \\ r &\triangleq \text{radius} \end{aligned}$$

The characteristic impedance is constant over the length of a uniform tube. However, at the *junction* of the 2 bronchi and the trachea, it changes, giving rise to partial reflection of incident traveling waves.

Pressure must be a continuous function everywhere, since otherwise a finite pressure drop would appear across a massless disk of air, resulting in infinite acceleration by Newton's second law of motion. Also, the sum of flows into the bronchi-trachea junction must be zero, assuming there is no loss there. We therefore have the following physical constraints at the junction:

$$\begin{aligned} P_1 &= P_2 = P_3 = P_J, \quad \text{and} \\ U_1 &+ U_2 + U_3 = 0. \end{aligned}$$

The total pressure at the junction is as follows:

$$P_J = \frac{2\sum_{i=1}^{3} \Gamma_i P_i^+}{\sum_{j=1}^{3} \Gamma_j} \tag{19}$$

and

$$P_k^- = P_J - P_k^+, \quad k = 1,2,3 \tag{20}$$

where the characteristic admittance $(\Gamma) = 1/Z$ is the reciprocal of the characteristic impedance Z. The admittance is calculated separately for each of the 2 bronchi (which are not always symmetrical) and the trachea.

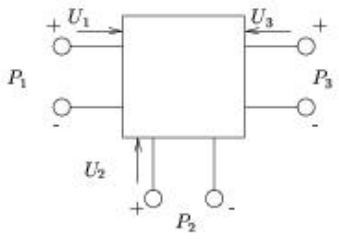

Figure 5: *3-Port Parallel Junction*.

The outputs of the three acoustic tube models are filtered to simulate pressure-wave losses due to traveling across the length of the tube. The frequency response of each filter approximates

$$\beta_k(\omega) = e^{-\alpha_k(\omega) L_k}$$

where $\alpha_k(\omega) = 2 \times 10^{-5} \sqrt{\omega} / A_k$ m^{-1} is imaginary part of the wavenumber per meter [5].

Radiation losses at the beak are accounted for using another lowpass filter (LPF), the output of which is negated to simulate the reflection of an open end tube.

4. CONCLUSIONS AND FUTURE WORK

The output of the model is the voiced sound produced by the vibrating membranes in the syrinx. It is very rich in harmonics, unlike the purer flute-like tone associated with the songbird.

The aim of this research is to create a computer musical instrument—one that is based on a physical model with physical parameters that can be manipulated to control the produced sound in an intuitive manner. While we desire initially to keep the model as close as possible to scientific reality, we hope also to explore an extended range of sound synthesis possibilities based on avian acoustic mechanisms.

REFERENCES

[1] M. R. Ballintijn and C. T. Cate. Sound production in the collard dove: A test of the 'whistle' hypothesis. *Journal of Experimental Biology*, 201:1637–1649, 1998.

[2] J. Brackenbury. *Form and Function in Birds*, chapter Functions of the syrinx and control of sound production, pages 193–220. New York Academic Press, 1989.

[3] N. H. Fletcher. Bird song – a quantitative acoustic model. *Journal of Theoretical Biology*, 135:455–481, 1988.

[4] N. H. Fletcher. *Acoustic Systems in Biology*. Oxford University Press, New York, New York, 1992.

[5] N. H. Fletcher and A. Tarnopolsky. Acoustics of the Avian Vocal Tract. *Journal of the Acoustical Society of America*, 105(1):35–49, January 1999.

[6] N. H. Fletcher. Private email correspondence, July 2002.

[7] N. H. Fletcher and T. D. Rossing. *The Physics of Musical Instruments*. Springer-Verlag, 1995.

[8] F. Goller and O. N. Larsen. *In Situ* biomechanics of the syrinx and sound generation in pigeons. *Journal of Experimental Biology*, 200:2165–2176, 1997.

[9] A. S. King. *Form and Function in Birds*, chapter Functional Anatomy of the Syrinx, pages 105–191. New York Academic Press, 1989.

[10] J. O. Smith. Discrete-time lumped models. www-ccrma.stanford.edu/~jos/NumericalInt/, May 2002. Course notes for MUS421/EE367B, Stanford University.

[11] J. O. Smith. Wave digital filters. www-ccrma.stanford.edu/~jos/WaveDigitalFilters/, March 2002. Course notes for MUS421/EE367B, Stanford University.

[12] J. O. Smith. Digital Waveguide Modeling of Musical Instruments. www-ccrma.stanford.edu/~jos/waveguide/, May 9, 2002.